EFFECT OF FREE-STREAM TURBULENCE ON FLUID FLOW AND HEAT TRANSFER FROM SQUARE CYLINDER

Ranjan P.*, Dewan A. and Kumar S.
*Author for correspondence
Department of Applied Mechanics
Indian Institute of Technology Delhi
New Delhi – 110016, India
E-mail: amz128264@am.iitd.ac.in

ABSTRACT

Simulations were carried out to study the effect of free-stream turbulence (FST) on forced convection from a heated square cylinder in a cross-flow. The computations were performed using LES methodology with the dynamic Smagorinsky model used for the sub-grid stress modelling. The values of the inlet turbulence intensity considered were 4, 8 and 12% at a Reynolds number of 16000. It has been observed that the mean drag and pressure coefficient increases with inlet turbulence, but the Strouhal number remains unchanged. Heat transfer from the side faces increases sharply with inflow turbulence than that at the back face. The rise in *Nu* for rear face is approximately 15% compared to 35% rise for the side face from the smooth flow to 12% FST case.

INTRODUCTION

Heat transfer from a bluff body kept in a cross-flow is one of the majorly encountered practical problems. In many practical situations, the incoming flow is turbulent and it may significantly affect the fluid and thermal behaviors around the rectangular cylinder. The free-steam turbulence present in the incoming flow may increase the momentum transfer around the cylinder which can interfere with the separated shear-layer thus changing the flow and heat transfer characteristics. Therefore, it becomes important to study the effect of the free-stream turbulence on heat transfer from rectangular cylinders.

Fluid flow behavior around rectangular cylinders under free-stream turbulence condition was studied by many researchers. Majority of such studies dealt with basic experimental investigations. Lee [1,2] performed experiments to study the effects of incoming turbulence on 2-dimensional square prism. He varied the turbulence intensity (Iu) from 0 – 12% and studied its effect on the surface pressure on the cylinder. He observed that the mean base pressure coefficient (C_{pb}) rose with an increase in turbulence intensity but substantial change could only be observed for $Iu \geq 6\%$. Apart from the base pressure increase, pressure recovery on the side faces (face parallel to the stream direction) was also observed, which was attributed to thickening of shear-layer on the side faces due to high momentum transfer because of high turbulence. Petty [3] investigated the effects of scale of turbulence for flow past square prisms. He observed that, the base pressure coefficient varied significantly w.r.t. to Iu, increased by approximately 40% for Iu = 12% compared to a smooth flow. He observed a slight decrease in the base pressure coefficient when intensity was increased beyond 12%. Further, he also found out that at higher values of Iu there was no significant effect of turbulent length scale (Lu) on the base pressure coefficient. But, at lower values of Iu the base pressure coefficient did tend to increase with Lu, and a maximum variation of approximately 10% was observed.

The effects of incoming turbulence on the mean flow past two-dimensional rectangular cylinders were studied by [4]. They studied the combined effects of intensity and length scale of turbulence on the mean flow. They observed that for a rectangular cylinder with a low cross-sectional aspect ratio (R < 0.6) the mean C_{pb} did not vary much for low Lu but increased sharply from Lu/D = 0.8 to 2 after which it again started decreasing with increasing length scale. For the square cylinder, R = 1, no variation in C_{pb} was observed w.r.t. to Lu/D up to the value of 2, but afterwards as the value of Lu was increased the mean C_{pb} started decreasing very steeply. They observed that, it was surprising that the mean C_{pb} did not vary with Lu up to the value of 2. Laneville [5] presented similar results as by Nakamura and Ohya (1984) for a square cylinder and stated that the vortex shedding, mean C_{pb} and C_D, get affected by the turbulent length scale but at very high values (Lu/D > 3). He also concluded that the results cannot be relied as the effect of the blockage ratio would be large at larger length scales.

Saathoff and Melbourne [6] studied the effect of FST on a square cylinder for higher range of turbulent intensity up to 24% with turbulent length scale of the order of 1D. They observed that, the fluctuating pressure coefficient $\left(C_p'\right)$ on the streamwise face reached a maxima at $Iu \approx 5\%$ and then decreased with increasing intensity up to $Iu \approx 12\%$. They further observed that as the turbulence intensity approached a value of 20%, the C_p' increased but the pressure fluctuated over a broader frequency range suggesting the interference of FST on the vortex shedding process. A detailed study of the effect of FST on instantaneous pressure field for flow over a rectangular cylinder was carried out by [7]. They carried out experiment at Iu = 5.3% and observed that there was not much difference between the power spectra of instantaneous pressure for smooth and turbulent flows for the case of a square cylinder. This behavior was due to the fact that the whole streamwise face was inside the separated shear-layer region and the turbulent intensity was very low to have any significant effect. All the above-mentioned studies were experimental and the free-stream turbulence was generated

using square-mesh biplanar grids of rectangular-section bars. FST generated using this technique is physical, but it is quite difficult to decouple the intensity and length scale of the generated turbulence. Hence, it becomes difficult to exclusively study the effect of intensity or length scale of turbulence on flow dynamics. Therefore, computational approach can be used to separately study the effect of different intensities or length scale of FST on flow field.

Many researchers have attempted to computationally study the effect of the free-stream turbulence for different flow configurations using various turbulence models. Initially, many standard RANS models and their variants were used [8–10] to study the effects of FST on boundary-layers. They all observed that, for lower FST values (Iu < 5%) these models provided reasonable predictions of the skin friction coefficient and Stanton number. But, for large turbulence intensity these models failed to predict the correct flow physics and an error as high as 50% was reported in terms of turbulence kinetic energy at $Iu \approx$ 20%. The main reason for this type of behavior can be attributed to the fact that, turbulence present in the free-stream has a significant effect on the production and transportation of turbulence kinetic energy. This effect is, however, not considered in all RANS or algebraic stress models. Based on these studies it is clear that higher modelling strategies are required to account for the effects of the free-stream turbulence. Recently few studies [11–13] based on Large Eddy Simulation (LES) were carried out to study the boundary-layer growth on a flat plate in the presence of the free-stream turbulence and the predictions compared well with the experimental results. Hence, it can be said that the LES methodology is appropriate to study the effect of free-stream turbulence.

Some recent LES studies were performed for flow over square cylinders [14–16]. Boileau et al. [15] and Cao and Tamura [16] demonstrated the applicability of LES with unstructured grids and showed that LES model can be used for various complex geometric configurations where making a structured grid is difficult. Liu [17] and Fang et al. [18] studied the effect of a homogenous turbulent flow on a square cylinder. Liu [17] used a digital filtering technique, namely, auto regressive moving average (ARMA) model, to generate the free-stream turbulence with turbulent intensity of 5% and length scale of 0.5D. He observed that, inflow with turbulence generated random characteristics in instantaneous lift and drag coefficients over a wide range of frequencies. Similarly, [18] also observed that the fluctuating lift and drag coefficients increased with turbulent intensity varying from smooth to 5 or 10%.

Based on the above-mentioned literature survey, it can be concluded that there is a need to perform a detailed study of the effect of FST for flow over a square cylinder. Further no study on heat transfer under turbulent inflow conditions has been reported in the literature. Hence, in this paper fluid flow and heat transfer characteristics from a square cylinder under homogenous inflow turbulence condition have been studied. The turbulence intensity was varied up to 12% and turbulent length scale was kept constant at 0.75D.

NUMERICAL METHOD

To study the effect of FST on flow and heat transfer characteristics from a square cylinder, large eddy simulation is used as turbulence modelling strategy. The dynamic Smagorinsky model is used to consider the sub-grid stress tensor. The computational domain for this study is shown in Figure 1. The meshing strategy used should be able to resolve the free-stream turbulence generated at the inlet. The grid was generated using the commercial software ANSYS-ICEM. Very close to the cylinder, as the $y+$ values are to be maintained below 1, the mesh size was kept equal to 0.01D and the first cell height from the cylinder was maintained below $0.1D/\mathrm{Re}^{0.4}$. From the cylinder, the cell growth rate was maintained at 1.02 in the radial direction. At the outer boundaries the grid size was kept approximately equal to 0.1D, so as to maintain the grid size below the Taylor micro-scale of the generated turbulence at the inlet. In the spanwise ($\Delta z+$) and streamwise ($\Delta x+$) directions the non-dimensional mesh sizes were varied in the ranges of 10 - 120 and 1 - 40, respectively.

The simulations are carried out at a Reynolds number of $1.6\text{x}10^4$ and the free-stream turbulence intensity was varied from 4% to 12% keeping the turbulent integral length scale constant at 0.75D. The temperature difference between the cylinder and free-stream was maintained at 30°, so that temperature behaved as a scalar quantity. The boundary conditions used are shown in Figure 1.

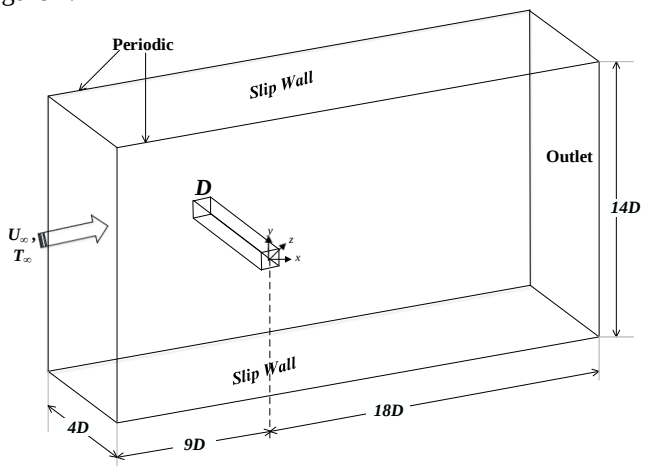

Figure 1 Computational domain considered in the present study.

FREE STREAM TURBULENCE GENERATION

To study the effect of FST on flow over cylinder, it is quite important to generate a time varying turbulent velocity field at the inlet. The most accurate method to achieve the inlet turbulence is to perform a precursor simulation. Thereafter a time varying data generated from the precursor simulation is mapped with the inlet of the actual simulation. However, this method is computationally expensive as it is limited to small computational domain and requires a large storage to save the data from a precursor simulation. To overcome this weakness many researchers have proposed various methods to generate synthetic turbulence. However, the challenge is to synthetically generate a turbulent field which will follow the physical turbulence. In the

present study, a method suggested by Davidson [19] is used and is briefly described here. A turbulent velocity field can be simulated using random Fourier modes. The velocity field is given by *N* random Fourier modes as

$$u_i'(x_j) = 2\sum_{n=1}^{N} \hat{u}^n \cos(\kappa_j^n x_j + \psi^n)\,\sigma_i^n$$

where $\hat{u}^n$, ψ^n and σ_i^n are the amplitude, phase and direction of Fourier mode *n*, respectively. The highest wave number was chosen based on the mesh resolution $\kappa_{max} = 2\pi/2\Delta$, where Δ is the grid spacing. The fluctuations were generated on a grid with equidistant spacing, $\Delta\eta = y_{max}/N_j$, $\Delta z = z_{max}/N_k$, where η denotes the wall-normal direction and N_j and N_k denote number of cells in the *y* and *z* directions, respectively. The fluctuations were set to zero at the wall and were then interpolated to the inlet plane of the CFD grid (the *y*-*z* plane).

The smallest wave number was defined from the expression $\kappa_1 = \kappa_e/p$, where $\kappa_e = \alpha 9\pi/55L_t$, α = 1.453. The factor p should be larger than one to make the largest scales larger than those corresponding to κ_e. In the present study p = 2 was considered. Thereafter the wave number space was divided into *N* modes, equally large of size $\Delta\kappa$. A modified von Karman equation was then chosen to calculate the energy associated with different wave numbers. This equation follows von Karman spectrum and is given by

$$E(\kappa) = \alpha \frac{u_{rms}^2}{\kappa_e} \frac{(\kappa/\kappa_e)^4}{[1+(\kappa/\kappa_e)^2]^{17/6}} e^{\left[-2(\kappa/\kappa_\eta)^2\right]}$$

$$\kappa = (\kappa_i\kappa_i)^{1/2}, \qquad \kappa_\eta = \varepsilon^{1/4}\nu^{-3/4}$$

Hence the amplitude was obtained by the expression $\hat{u}^n = \left(E(|\kappa_j^n|)\Delta\kappa\right)^{1/2}$. Further, from the continuity equation it is known that the unit vector σ_i^n and κ_j^n are orthogonal. σ_3^n can be arbitrarily chosen such that it is parallel to κ_i^n. Thus with $\hat{u}^n$, κ_j^n, ψ^n and σ_i^n known the fluctuations can be determined.

As the fluctuating field was generated at every time step, velocities were not correlated and were rather independent which is unphysical. To create correlation in time, new fluctuating velocity fields u_i' were computed based on asymmetric time filter

$$(u_i')^m = a(u_i')^{m-1} + b(u_i')^m$$

where, *m* denotes the time step number, $a = \exp(-\Delta t/\mathrm{T})$ and $b = (1 - a^2)^{0.5}$. Hence the time correlation obtained was equal to $\exp(-\Delta t/\mathrm{T})$ and the total velocity at the inlet was obtained as

$$\bar{u}_i(0,y,z,t) = U_i(y) + u_i'(y,z,t)$$

where, $\bar{u}_i$ is the total velocity, U_i the mean velocity and $u_i' = (u_i')^m$. In our case $U_2 = U_3 = 0$ and therefore the total velocity in the cross and span directions were equal to the fluctuating part only. The free-stream turbulence generated still need to be tested. The free-stream turbulence generation technique described in Section 7.2 needs to be validated for its effective application. Davidson [19] validated the technique for a flow inside a channel for a turbulent Reynolds number of 500. He compared the results between the synthetically generated inlet turbulence with DNS generated fluctuating inlet from a precursor simulation and observed that both the techniques of generating inlet turbulence were comparable to each other within 5%.

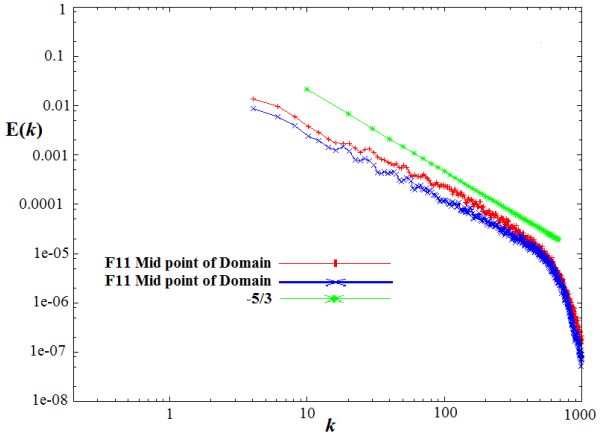

Figure 2 Power spectrum of streamwise and cross-stream velocity fluctuations compared with the von Karman energy spectrum.

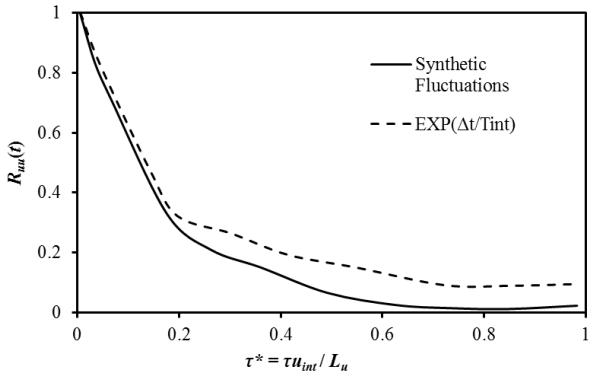

Figure 3 Autocorrelation of streamwise fluctuating velocity. T_{int} is the integral time scale of the generated FST, u_{int} is the integral velocity scale, which is equal to the required fluctuating velocity, and L_u the integral length scale.

RESULTS AND DISCUSSIONS

Grid Independence Study

It is important to test the sensitivity of the numerical setup towards the grid resolution. In the present LES study, grid filter was used and hence it becomes difficult to perform a grid independence study. But, it is important to use a mesh size which is independent in terms of predicting the mean flow features. For, this purpose four different cases were considered to study the effect of grid size and these are summarized in Table 1. To study the grid sensitivity, inlet with no free-stream turbulence was considered and aerodynamic properties and mean pressure coefficient around the cylinder were plotted.

Table 1 Study of grid resolution sensitivity.

S.No	Grid Size	*y+*	$\overline{C_d}$	C_l'	*St*	$-C_{pb}$
1	200×150×40	≤ 1.32	2.24	1.15	0.135	1.38
2	300×200×60	≤ 1.32	2.20	1.35	0.131	1.35
3	300×300×60	≤ 1.32	2.19	1.37	0.130	1.35
4	300×300×80	≤ 0.98	2.20	1.37	0.131	1.36

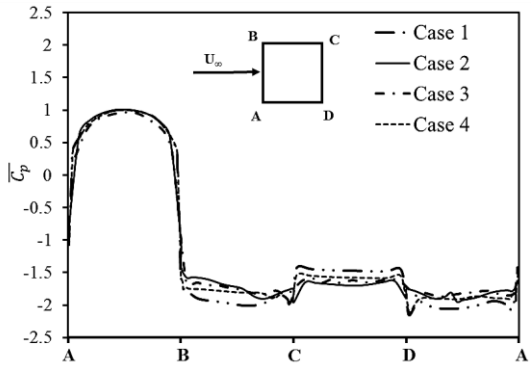

Figure 4 Mean pressure coefficient around the cylinder.

It can be observed from Table 1, which presents the aerodynamic statistics, and Figure 4, which shows the mean pressure coefficient, that there is not much difference in the results between various grid resolutions. Hence mesh size of Case 2 can be considered for the rest of the study. An important issue which needs to be considered for the grid independence study is the grid size near the cylinder and its growth factor in the radial direction from the cylinder as described in the previous section (Numerical Method). Hence, the possibility of using a very coarse mesh is difficult and the mesh size in the cross-stream and span directions can only be changed.

Effect of FST on Pressure and Aerodynamic Properties

The computations were carried out with the grid size of Case 2 as given in Table 1. A total of four simulations were carried out, one with no inflow turbulence and other three at the free-stream turbulence intensities of 4, 8 and 12%. The length scale of the incoming turbulence was kept constant at 0.75*D*. The results were normalized by various scales of motions: length by the cylinder diameter *D*, velocity by the free-stream velocity U_∞ and time by the flow time (t_f) defined as the time taken to travel from the inlet of the domain to the outlet at the free-stream velocity.

Figure 5 shows variation of mean pressure coefficient around the periphery of the square cylinder. It can be noted that variation of the mean pressure on the front face is minimal w.r.t. to the turbulent intensity. The reason for this behavior can be attributed to the stagnation zone and the laminar boundary-layer formed on the front face which is largely unaffected by the FST. A major difference can be observed for the side faces (top B-C and bottom D-A) and the rear face (C-D). It can be observed that there is not much difference between the smooth flow and FST with 4% intensity, but as the intensity is increased, the mean pressure coefficient recovers very strongly towards the trailing edge of the cylinder. This recovery then leads to a higher pressure coefficient on the rear face also. The recovery of pressure towards the trailing edge of the cylinder and on the rear face can be attributed to the fluctuating flow components which thicken the separated shear-layer by entraining the fluid from the mean flow. Further the R.M.S pressure coefficient (C_p') around the cylinder is also plotted in Figure 6. At the front face, as the intensity of the inflow turbulence is increased, the value of the R.M.S. pressure coefficient increases, with minima at the center of the face and it increases towards the corners as the flow accelerates towards the corners. An important observation that can be made here is that on the side face and on the rear face the values of C_p' are lesser for the cases with inflow turbulence than for smooth flow, rather these decrease as the inlet intensity is increased (Figure 6).

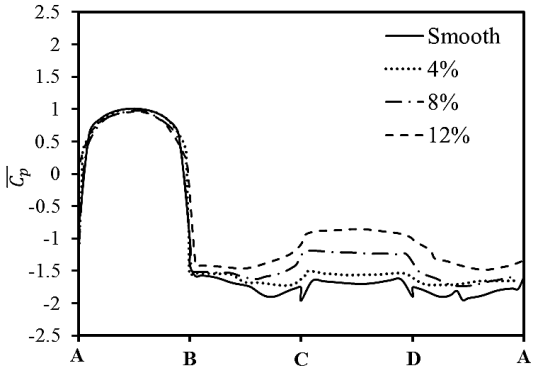

Figure 5 Mean pressure coefficient around the cylinder. Please see Figure 4 for *x*-axis labeling.

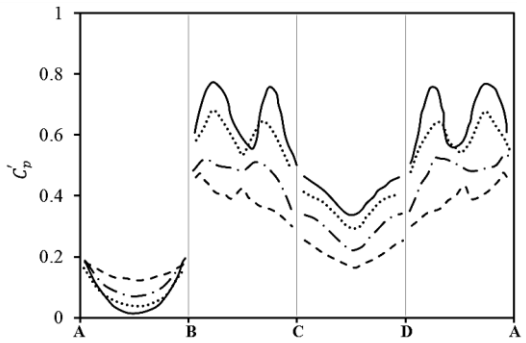

Figure 6 R.M.S pressure coefficient around the cylinder. Please see Figure 4 for *x*-axis labeling.

This behavior is in contrast to the mean pressure coefficient and it can be explained as follows. In a smooth flow, the flow gets separated from the leading edge and forms the vortex street very close to the rear face, due to which a high level of turbulence is experienced at the trailing corners and on the rear face. When the fluctuation is added to the incident flow, it basically entrains the fluid from the surrounding fluid thus causing the separated shear-layer to bend inwards causing intermittent reattachment on the side face. This behaviour results in the shifting of the vortex street far from the rear face in the downstream direction hence resulting in a lower level of pressure fluctuation on the rear face.

The distribution of C_p' on the side face also presents an important flow physics. The two peaks seen in Figure 6 on the side face are due to the rolling of the center of the separation bubble over a vortex cycle from 0.25*D* to 0.75*D* from the leading edge. As the inflow turbulent intensity is increased, due to an inward bending of the separated shear-layer, the second peak gets shifted upstream and for 12% FST it is nearly at the center of the side face. The fluid entrainment, due to an increased level of turbulence, reduces the magnitude of peaks in C_p' on the side face (Figure 6).

The power spectral density (PSD) of pressure on side and rear faces is plotted in Figures 7and 8. Two points at which pressure

is measured on the side face are located at 0.1D and 0.9D from the leading edge corner. For the rear face, the two points are at 0.1D and 0.5D from the top trailing edge at which pressure is measured. It can be observed from the PSD of the side face (Figure 7) that close to the leading edge the power spectra is not much influenced by the inflow turbulence, but towards the trailing edge there is a large difference between the three cases. It can be observed that for higher inflow turbulence intensity the power spectra is more distributed thus showing other dominant frequencies of the vortex shedding. This behavior shows that, turbulence present in the free-stream distributes the energy over a wider range of frequency thus reducing the strength of the vortex shedding. Similarly, for the rear face, as the inlet turbulent intensity increases the contribution from lower frequencies also increases thus reducing the magnitude of the dominant peak at the shedding frequency. This contribution is due to slow oscillations of the recirculating flow just downstream of the cylinder.

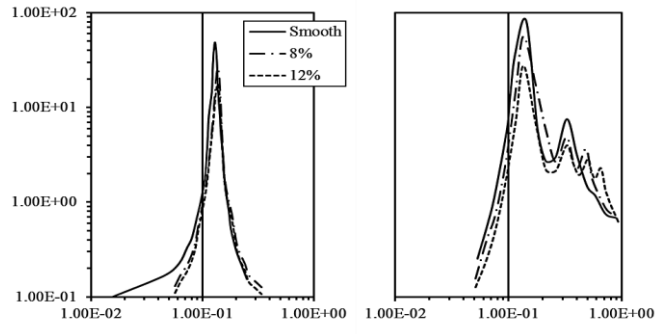

Figure 7 Power spectral density of pressure on side faces at two points: (a) 0.1D from the leading edge and (b) 0.9D from the leading edge.

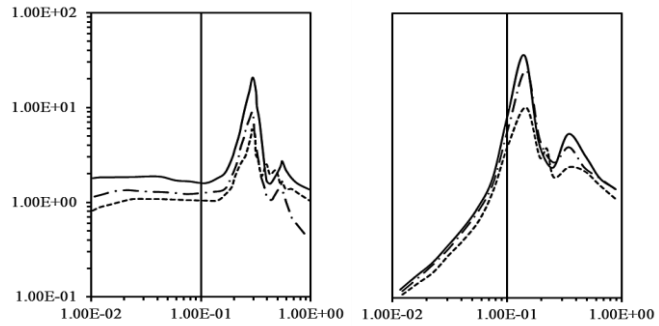

Figure 8 Power spectral density of pressure on rear faces at two points: (a) 0.5D from the trailing edge top corner and (b) 0.1D from the trailing edge top corner.

It can be observed from the above discussion, that there is a significant variation in pressure w.r.t. the inlet turbulent intensity and hence there will be variations in aerodynamic properties. Figure 9 shows variations in the mean drag coefficient($\overline{C_D}$), mean base pressure coefficient $\left(\overline{C_{pb}}\right)$ and fluctuating lift coefficient $\left(\overline{C_l'}\right)$ w.r.t. the inlet turbulent intensity. The mean drag and base pressure coefficients complement each other; as the value of I_u increases the base pressure coefficient rises and thus the drag coefficient reduces with I_u. The rise in $\overline{C_{pb}}$, as already discussed, is due to a higher rate of fluid entrainment from the surroundings. Further, it can be observed that the fluctuating lift coefficient decreases with I_u. The reason for this behavior can be attributed to a weakening of the vortex shedding strength due to a shift in the vortex formation far from the cylinder rear face as already explained.

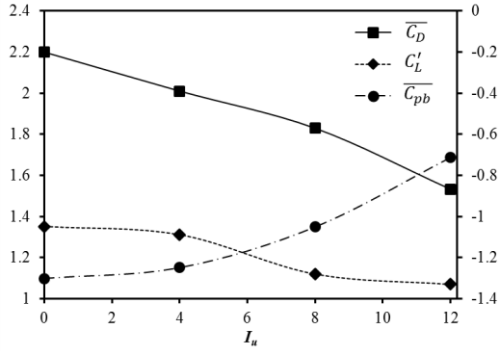

Figure 9 Variation of aerodynamic properties w.r.t. to inlet turbulence intensity: for $\overline{C_D}$ and $\overline{C_l'}$ see left vertical axis and for $\overline{C_{pb}}$ right vertical axis.

Time histories of both drag and lift coefficients are plotted in Figures 10 and 11. It can be observed that a large amount of random characteristics are present in the time history of drag and lift coefficients, which are due to the presence of inlet free-stream turbulence. For the FST case, the lift coefficient plot (Figure 11) shows area of varied higher frequencies suggesting the presence of randomly distributed eddies. The drag coefficient plot shows more random characteristics and the fluctuations are also large for 12% FST case compared to the smooth flow case (Figure 10).

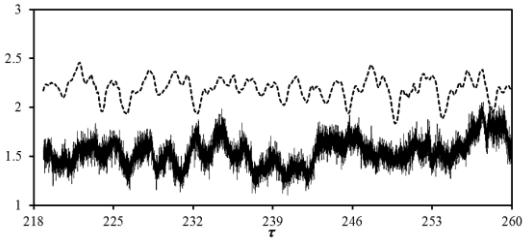

Figure 10 Time history of drag coefficient for smooth flow: dotted line, and FST flow with 12% intensity: solid line.

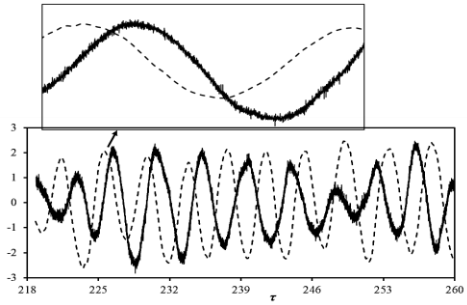

Figure 11 Time history of lift coefficient for smooth flow: dotted line, and FST flow with 12% intensity: solid line. Expanded view is also shown.

Effect of FST on Heat Transfer

The effects of inflow turbulence on flow dynamics for flow over square cylinder were presented in the previous section. An attempt is made in this section to understand the physical aspects of heat transfer distribution.

Figure 12 shows variation in the time-averaged global Nusselt number (*Nu*). To calculate the global Nusselt number, first time averaging is performed and then the time averaged values of *Nu* are averaged around the cylinder. Figure 12 shows that the value of the global *Nu* steadily increases with the inlet turbulent intensity. A rise of approximately 24% is observed for the 12% FST case compared to the smooth flow case. The reason for this increase in *Nu* can be found by plotting the time-averaged local Nusselt number around the cylinder.

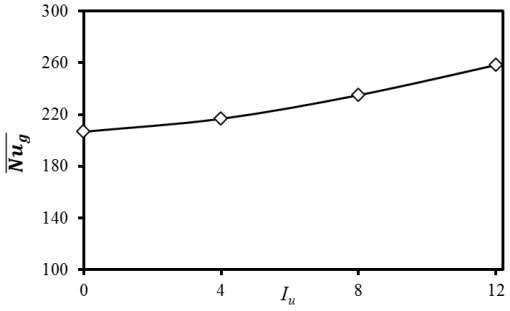

Figure 12 Time averaged global Nusselt number w.r.t. inlet turbulent intensity.

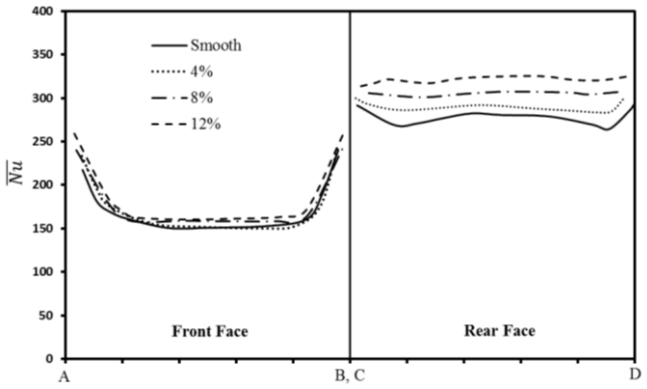

Figure 13 Time-averaged Nusselt number along the front and rear faces for different FST values.

The time-averaged local *Nu* along the front and rear faces is plotted in Figure 13 and Figure 14 shows variations along the side faces for different FST conditions. At the front face, similar to the mean pressure coefficient, there is not much change in values of *Nu* for different FST cases. This behavior is due to the stagnation point encountered by the fluid, where the Nusselt number is the lowest. The Nusselt number then increases towards the leading corners of the cylinder as the flow accelerates towards the corners thus increasing the mean velocity gradient which in turn increases the heat transfer.

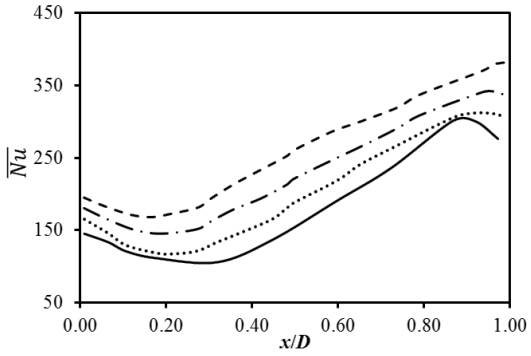

Figure 14 Time-averaged Nusselt number along the side face for different FST values (legends same as in Figure 13).

The Nusselt number profile on the side face is interesting, as there is a small difference between the smooth flow case and 4% FST case, but the profile of *Nu* for higher FST cases is different close to the trailing edges of the cylinder (Figure 14). This behavior is due to an inward bending and intermittent reattachment of the separated shear-layer on the side face which causes the heat transfer to increase further at the trailing edges of the cylinder as compared to the smooth flow case, where *Nu* drops very close to the trailing edge. It can be observed that *Nu* increases by approximately 35% for 12% FST case compared to the smooth flow case for the side face (Figure 14). Due to this increase in *Nu* at the side faces a large variation in *Nu* for the rear face is also expected with increasing FST. But Figure 13 shows that increase in the value of *Nu* is not steep for the rear face for different FST conditions. The reason behind this behavior is the stretching and formation of vortex street away from the cylinder rear face due to which the turbulence level drops which affects the heat transfer in that region. Another important observation is the loss of shape "W" on the rear face as the inlet turbulent intensity is increased, which is because of varied structures present in that region at wider range of frequencies.

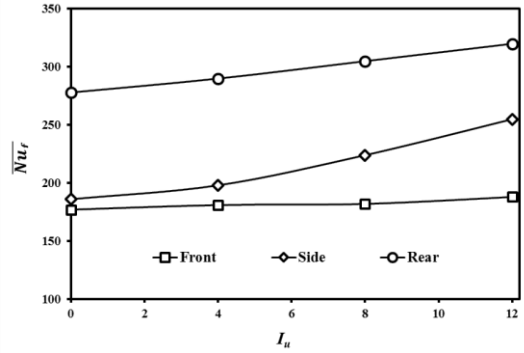

Figure 15 Face-averaged Nusselt number w.r.t. different FST conditions.

Further, the face-averaged Nusselt number for all the faces is also plotted w.r.t. the inlet turbulent intensity (Figure 15). As already discussed, variation in *Nu* for the front face is minimal and maximum for the side face. The rise in *Nu* for the rear face is approximately 15% compared to 35% rise for the side face from the smooth flow case to 12% FST case.

CONCLUSION

Flow and heat transfer behavior of a free-standing square cylinder in a cross-air stream with free-stream turbulence are studied. The turbulent integral length and velocity scales were defined and simulations were performed. The length scale was kept constant at 0.75*D* and the fluctuating intensity was varied from 0 to 12%. The major conclusions of this study are

1. The mean pressure and fluctuating pressure coefficients are plotted around the cylinder. While the mean pressure coefficient increases with increasing turbulent intensity, the fluctuating pressure decreases.
2. The base pressure coefficient also increases with increasing free-stream turbulence hence reducing the mean drag coefficient.
3. Power spectra of pressure shows that, as the inflow turbulence increases, the power spectrum gets wider because of the distribution of energy in higher frequency range. This in turn reduces the strength of the vortex shedding.
4. As expected, the heat transfer from the cylinder is increased with increasing turbulent intensity at the inlet, but the major changes are only observed at the side faces.
5. At the rear face, due to a reduction in the strength of the vortex street, the heat transfer is not as enhanced as on the side face.

REFERENCES

[1] B.E. Lee, The effect of turbulence on the surface pressure field of a square prism, J. Fluid Mech. 69 (1975) 263–282. doi:10.1017/S0022112075001437.

[2] B.E. Lee, Some effects of turbulence scale on the mean forces on a bluff body, J. Wind Eng. Ind. Aerodyn. 1 (1975) 361–370. doi:10.1016/0167-6105(75)90030-6.

[3] D.G. Petty, The effect of turbulence intensity and scale on the flow past square prisms, J. Wind Eng. Ind. Aerodyn. 4 (1979) 247–252. doi:10.1016/0167-6105(79)90005-9.

[4] Y. Nakamura, Y. Ohya, The effects of turbulence on the mean flow past two-dimensional rectangular cylinders, J. Fluid Mech. 149 (1984) 255–273. doi:10.1017/S0022112084002640.

[5] A. Laneville, Turbulence and blockage effects on two dimensional rectangular cylinders, J. Wind Eng. Ind. Aerodyn. 33 (1990) 11–20. doi:10.1016/0167-6105(90)90016-6.

[6] P. Saathoff, W.H. Melbourne, Effects of freestream turbulence on streamwise pressure measured on a square-section cylinder, J. Wind Eng. Ind. Aerodyn. 79 (1999) 61–78. doi:10.1016/S0167-6105(98)00112-3.

[7] H. Noda, a. Nakayama, Free-stream turbulence effects on the instantaneous pressure and forces on cylinders of rectangular cross section, Exp. Fluids. 34 (2003) 332–344. doi:10.1007/s00348-002-0562-0.

[8] P. Bradshaw, Effect of free-stream turbulence on boundary layer, in: AFOSR-HTTM Stanford Conf. Complex Turbul. Flows, Thermo-Sciences Division, Mechanical Engineering Department, Stanford University, Stanford, CA, 1981: pp. 86–93.

[9] A.M. Savill, Algebraic and Reynolds Stress Modeling of Manipulated Boundary Layers Including Effects of Free-Stream Turbulence, in: Proc. R. Aeronaut. Soc. Int. Conf. Turbul. Drag Reduct. by Passiv. Means, London, UK, 1987: pp. 89–143.

[10] G.R. Iyer, S. Yavuzkurt, Comparison of low Reynolds number k–ε models in simulation of momentum and heat transport under high free stream turbulence, Int. J. Heat Mass Transf. 42 (1999) 723–737. doi:10.1016/S0017-9310(98)00194-X.

[11] K. Liu, R. Pletcher, A Large Eddy Simulation of a Turbulent Boundary Layers Subjected to Free-Steam Turbulence, in: 43rd AIAA Aerosp. Sci. Meet. Exhib., American Institute of Aeronautics and Astronautics, Reston, Virigina, 2005. doi:10.2514/6.2005-669.

[12] G.L. Lioznov, V.G. Lushchik, M.S. Makarova, a. E. Yakubenko, Freestream turbulence effect on flow and heat transfer in the flat-plate boundary layer, Fluid Dyn. 47 (2012) 590–592. doi:10.1134/S0015462812050055.

[13] Q. Li, P. Schlatter, D.S. Henningson, Simulations of heat transfer in a boundary layer subject to free-stream turbulence, J. Turbul. 11 (2010) N45. doi:10.1080/14685248.2010.521505.

[14] M.R. Nazari, A. Sohankar, S. Malekzadeh, A. Alemrajabi, Reynolds-averaged Navier–Stokes simulations of unsteady separated flow using the k−ω−υ2−f model, J. Turbul. 10 (2009) 1–13. doi:10.1080/14685240903241805.

[15] M. Boileau, F. Duchaine, J.-C. Jouhaud, Y. Sommerer, Large-Eddy Simulation of Heat Transfer Around a Square Cylinder Using Unstructured Grids, AIAA J. 51 (2013) 372–385. doi:10.2514/1.J051800.

[16] Y. Cao, T. Tamura, Large-eddy simulations of flow past a square cylinder using structured and unstructured grids, Comput. Fluids. 137 (2016) 36–54. doi:10.1016/j.compfluid.2016.07.013.

[17] Z. Liu, Investigation of Flow Characteristics Around Square Cylinder with Inflow Turbulence, Eng. Appl. Comput. Fluid Mech. 6 (2012) 426–446. doi:10.1080/19942060.2012.11015433.

[18] F. Fang, M.-W. Tsai, Y.-C. Li, The Effect of Turbulent Uniform Flow around A Square Cylinder, in: Proc. World Congr. Mech. Chem. Mater. Eng., Barcelona, Spain, 2015: pp. 294-1-294–7.

[19] L. Davidson, Using isotropic synthetic fluctuations as inlet boundary conditions for unsteady simulations, Adv. Appl. Fluid Mech. 1 (2007) 1–35.